Digest Journal of Nanomaterials and Biostructures Vol. 11, No. 2, April - June 2016, p. 615 - 624

STRUCTURAL AND MORPHOLOGICAL EVOLUTIONS INDUCED BY THE ANNEALING OF CaF_2 NANOCRYSTALLINE POWDERS BY USING Eu^{3+} ION PROBE LUMINESCENCE

S. POLOSAN, M. SECU, M. ENCULESCU*
National Institute of Materials Physics, PO Box MG-7, 77125, Magurele-Bucharest, Romania

Eu-doped CaF_2nanocrystalline powders have been prepared by using co-precipitation technique. Structural and morphological modifications induced by annealing are followed by using Eu^{3+}-ion probe. Theluminescence properties are changing gradually together with the morphology of doped CaF_2 nanoparticles accompanied by an$Eu^{3+} \rightarrow Eu^{2+}$conversion. Cathodoluminescence measurements show uniform distribution of the europium dopant ions in the annealed samples accompanied by a strong increase of the integral photoluminescence signal. During annealing the cubic structure of CaF_2 nanoparticles is altered going to the spherical morphology due to the Eu^{3+} ions incorporation. In the annealed samples Eu^{3+} ions are incorporated as Eu^{3+}-O dimer centres with the coordination symmetry (C_{2v}); in the sintered samples there are two non-equivalent Eu^{3+} sites. The thermoluminescence peaks have been assigned to the recombination of the Eu^{3+} related traps in these sites.

(Received March 21, 2016; Accepted June 6, 2016)

*Keywords:*Eu-doped CaF_2, nano-crystals, photoluminescence, cathodoluminescence.

1. Introduction

Nanofluorides are one of the most important and large class of nanomaterials which are of keen interest to scientists due to their high potential for applications in various fields (optical amplifiers, optical waveguides, OLEDs, etc.) or life sciences related. Simple and complex nanofluorides of alkali earth metals doped with rare earth (RE)-ions showing efficient UP-conversion effects (i.e. near-infrared (NIR) conversion into the visible spectral range) [1-4] are opening up new alternative as fluorescent labels with great potential for imaging and biodetection assays in both in vitro and in vivo applications ([5] and references therein) or as novel antimicrobial and antibiofilm agents [6].Moreover, nanosizedthermoluminescent phosphors present an increase of the luminescence yield under high-dose irradiation and an improvement of radiation resistance [7]. Therefore in the last years there has been an increased interest toward the nanochemistry of the fluoride compounds new and various synthesis methods being proposed [8-10].

Among the fluoride compounds, CaF_2 is an important optical material with various applications for radiation detection (as scintillator and thermoluminescence dosimetry) or laser material because of its stability and non-hygroscopic behavior and its excellent properties such as high transmittance from ultraviolet to mid infrared spectral range, easy incorporation of RE-ions, low refractive index, high chemical resistance and high laser damage threshold. A viable and advantageous option over the crystal growth is the ceramics technology which is based on powders synthesis followed by subsequent refined treatments [11,12]; it is expected to replace single crystals, particularly in high-volume applications and those which need large gain media.Therefore in the last few years alternative methods have been proposed for the CaF_2 nanocrystals synthesis: hydrothermal [13], microwave-assisted hydrothermal route [14-15], co-precipitation [16] or non-aqueous routes [17].For ceramic technology related applications, powder processing is required

* Corresponding author: mdatcu@infim.ro

that might be accompanied by structural and morphological modifications. Hence for the luminescence efficiency improvement it is necessary an understanding of how the optical properties, in particular RE^{3+}-associated luminescence properties, are affected by further annealing and by the structural and morphological modifications induced.

The aim of the present work is to investigate the structural and morphological evolution induced by the thermal treatments of CaF_2nanocrystalline powders taking the advantages of Eu^{3+} ion to probe the site symmetry and based on group-theoretical arguments [18,19]. Additional methods as X-ray diffraction (XRD), scanning electron microscopy (SEM) and energy disperse X-ray analysis (EDX) are used for the evaluation of the structural and morphological properties.

2. Experimental

2.1. Samples preparation

For the synthesis of Eu^{3+}-doped CaF_2 nanoparticles(1 mol%) we used the co-precipitation method in a single-step solution-fluorination [16] with aqueous solutions of $Ca(NO_3)_2.4H_2O$ and NH_4F as starting materials added over $EuCl_3$ acid solution. The precipitation of solid Eu^{3+}-doped CaF_2 nanoparticles has been easily obtained by the reaction of theCa^{2+} and F^- ions that formed by the dissociation of $Ca(NO_3)_2$ and NH_4F in an aqueous solution. The resulted powder samples were carefully dried a 60^{o}C for several days followed by annealing at 800 and 1300^{o}C in open atmosphere. The high temperature (1300^{o}C) annealing yields to formation of $Ca(OH)_2$ additional phase and a degradation of the luminescence properties. Therefore we have used the sintering of the powder at 63 MPa and 1200^{o}Cin a graphite crucible.

2.2. Samples characterization

In order to study the thermal transformation of the powders, we performed thermogravimetric analysis (TG) and differential thermal analysis (DTA) using a TGA Instrument, model Pyris Diamond**,** Perkin Elmer Instruments, in the temperature range from 25 to 900°C with a heating rate of 10°C/min, in air.

The X-ray diffraction (XRD) measurements have been performed on a BRUKER D8 ADVANCE type X-ray diffractometer, in focusing geometry, equipped with copper target X-ray tube and LynxEye one-dimensional detector. The morphology of the powders was determined with a Carl Zeiss EVO 50 scanning electron microscope (SEM). The microscope is equipped with energy dispersive X-ray analysis (EDX) and cathodoluminescence accessories. The samples were placed on stabs using adhesive carbon discs. Previous to SEM evaluation a thin gold layer was sputterred on the structures. The distribution of europium was determined using energy dispersive X-ray analysis (Bruker).

Photoluminescence (PL) and PL excitation spectra have been recorded at room temperature using FS 920 Edinburgh Instruments spectrophotometer.The spectra were not corrected for the spectral sensitivity of the experimental set-up. The luminescent properties were also evaluated using cathodoluminescence.

Thermoluminescence (TL) measurements have been performed using a Harshaw 3500 TL reader, in the 50 to 400^{o}C temperature range using heating rate 1^{o}C/sec. Before the TL measurements the samples were X-ray irradiated at room temperature (RT) for 15 min. using a copper anode operating at 40 kV and 40 mA.

3. Results and discussion

The final solid solution of the Eu-doped CaF_2 nanocrystals with high concentration of dopant (high Eu/Ca ratio) can be formulated as $Ca_{1-x}Eu_xF_{2+x}$, in which the dopant enters with two valences, Eu^{2+} and Eu^{3+} respectively.

3.1.Thermal analysis

The thermal analysis (TG andDTA curves) of the "as prepared" europiumdoped CaF_2 powder are depicted in the Figure 1 and reveal the processes which take place during annealing. The consistent variation between 25 and 110^{o}C observed in both curves is assigned to the drying process of the powder. Starting with 350^{o}C up to 600^{o}C, a broad endothermic peak at 570^{o}C appears in DTA curve, accompanied by a small exothermic peak at 438^{o}C; the curve ends with an exothermic peak at 634^{o}C followed with a broad peak up to 900^{o}C.The shapes of both DTA and TG curves can be explained if we take into account the incorporation into the CaF_2 phase of both Eu^{2+} and Eu^{3+} ion species (confirmed also by PL measurements), besides other reaction products as NH_4NO_3 and NH_4Cl.

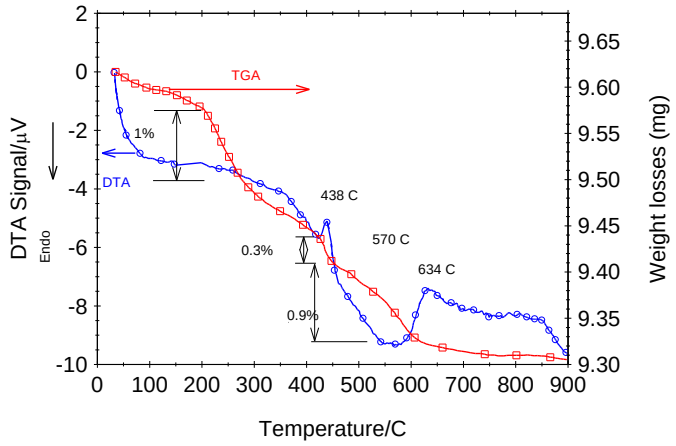

Fig. 1. Thermal analysis results for the 1 mol% Eu^{3+} doped CaF_2 "as-prepared" powder sample.

Since the PL measurements have shown the presence of the Eu^{2+} ions right after synthesis,this indicates a partial reduction of the trivalent europium ions. The concentration stability limits of solid solutions for CaF_2-EuF_2 systems reach the maximum value in the 400 to 600^{o}C range (in the melt) [20]. Therefore we suppose that the small crystallization peak at 438^{o}C in DTA curve (and the weight losses in the same region in TG curve) correspond to the thermally activated diffusion of the Eu^{2+} ions inside the CaF_2 nanocrystals with the formation of the $Ca_{1-x}Eu_xF_2$solid solution.The Eu^{2+}iongets inside the CaF_2 structure easierthan Eu^{3+} because it fulfils the Hume-Rothery rules and because EuF_2 has the same crystal structure and relative valence factor [21].

Because of the orthorhombic structure of EuF_3 and higher valence of Eu^{3+} compared with Ca^{2+} the incorporation of these ions requires higher energy (i.e. higher temperature) even if these ions have comparable ionic radii (1.21 Å for Eu^{3+} and 1.26 Å for Ca^{2+}).According to the Eu-F phase diagram that showed the formation of the α-EuF_3 compound above 600^{o}C [22], the exothermic peak at 634^{o}C has been assigned to the Eu^{3+} ions incorporation in the CaF_2 nanocrystals.

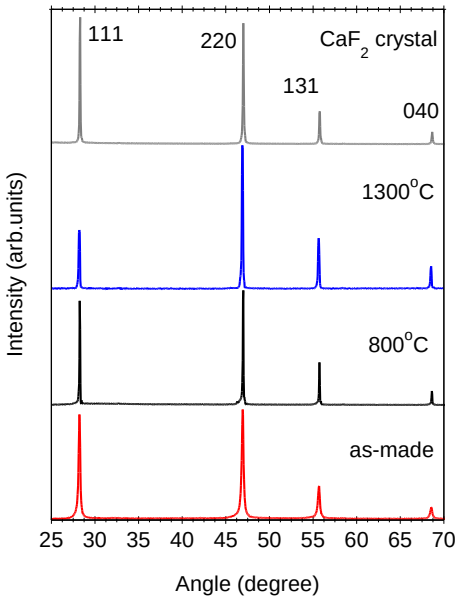

Fig. 2. XRD patterns of the "as-prepared", 800°C annealed, and 1300°C sintered samples. The XRD pattern of CaF_2 crystal is also shown for comparison.

3.2.X-ray diffraction

The XRD patterns of the "as-made" and annealed samples are depicted in the Figure 2. Comparison with the XRD pattern of a cubic-CaF_2 crystal showed the formation of the CaF_2 crystalline phase right after the chemical synthesis (Figure 2).During the high temperature annealing in air at 1300°C we observed the formation of $Ca(OH)_2$ additional phase (not shown) by replacing of some fluorine by hydroxyl ions which does not happen for sintered ceramic samples (Figure 2).

Assuming the particles are stress-free we used the broadening of the peaks in order to estimate the average nano-crystals size by using the Scherrer formula [23] applied to the (111) reflection of cubic CaF_2 at 28.0°. The mean size of the nanocrystals is below 100 nm in the "as-prepared" sample and increases to about 200 nm in the sample annealed at 800°C.

3.3.Scanning Electron Microscopy (SEM)

SEM images of the "as-prepared" and 800°C annealed samples presented in the Figure 3 (a, b) have showed agglomerated CaF_2 nanoparticles that prevent a reliable mean size determination; the presence of Eu dopant was confirmed by Electron Dispersed X-ray analysis (EDX). Nevertheless, in the "as-prepared" sample the nanoparticles size is below 100 nm while the particles are bigger in the annealed sample, i.e. between 150 and 200 nm, confirming the evaluation from XRD data. We noticed the spherical morphology which is consistent with the Eu^{3+} doping, compared to the undoped nanoparticles that show a cubic morphology [17]. The situation changes for the sintered sample where SEM image presented in Figure 3c shows a sample resembling with sintered ceramics.

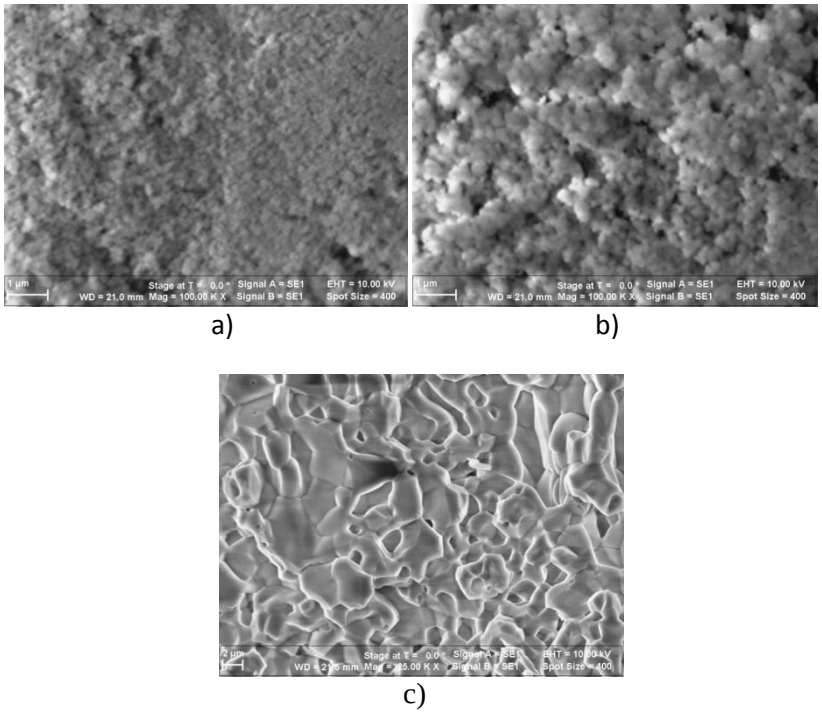

Fig. 3. SEM images of the Eu^{3+}-doped CaF_2 powder samples "as-prepared" (a), annealed at 800°C (b), and sintered at 1300°C (c).

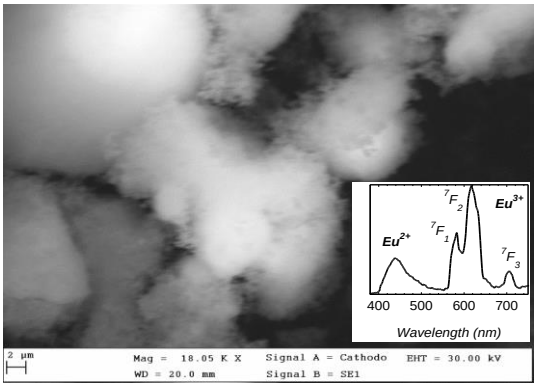

Fig. 4. CL image and CL spectrum (inset) of the Eu^{3+}-doped CaF_2 powder sample annealed at 800°C.

The cathodoluminescence (CL) image of the nanostructured Eu^{3+}-doped CaF_2 sample presented in Figure 4 confirms the uniform distribution of the emissive europium ions in the annealed powder. The CL spectrum (inset) shows emission peaks corresponding to transitions between the energy levels of both Eu^{2+} and Eu^{3+} ions.

3.4. Photoluminescence (PL) spectra

Luminescence processes are strongly influenced by the thermal treatments as can be clearly seen in the Figure 5 where are depicted the PL spectra excited at 394nm recorded on Eu^{3+}-doped as-prepared, annealed and sintered samples; the corresponding excitation spectra of the Eu^{3+}ions' associated emissions in different spectral domains are depicted in the Figure 6.

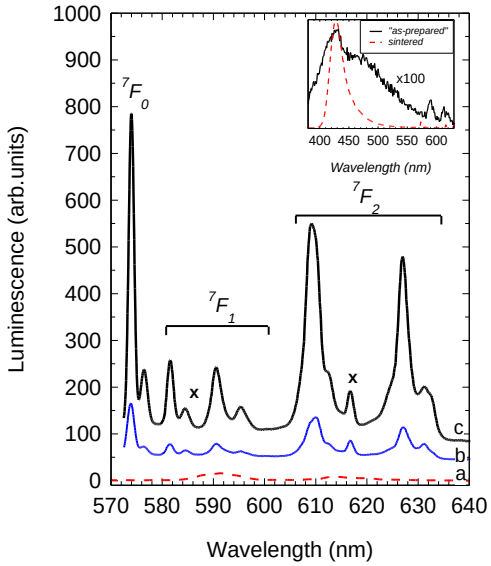

Fig. 5. Photoluminescence spectra recorded for Eu^{3+}-doped CaF_2 powder samples: "as-prepared" (curve a), annealed at 800°C (curve b) and sintered at 1300°C (curve c) samples using $\lambda_{ex.}$ = 394 nm excitation wavelength. The small peaks at 584nm and 616 nm are due to the $^5D_1 \rightarrow {}^7F_3$ and $^5D_1 \rightarrow {}^7F_4$ transitions, respectively. In the inset are shown the PL spectra recorded on "as-prepared" and sintered samples using UV excitation at 345 nm.

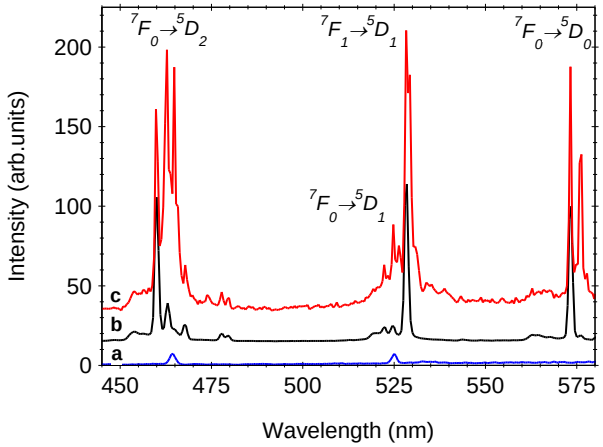

Fig. 6. PL excitation spectra of the photoluminescence at 620 nm recorded for Eu^{3+}-doped CaF_2 samples "as-prepared" (curve a), annealed at 800°C (curve b) and sintered at 1300°C (curve c).

PL spectra have shown strong luminescence in the visible range peaking at 578 nm, 591 nm, 612 nm, 650nm and 698nm assigned to the Eu^{3+}-ion transitions ($^5D_0 \rightarrow {}^7F_J$; J=1-4), accompanied by a broader band peaking at about 425 nm due to Eu^{2+} ions (Figure 5 – inset) [24]. In the annealed and sintered samples a clear Stark splitting of the PL bands appears due to the degeneracy level removal by the crystal field of the CaF_2 structure where the Eu^{3+}-ions are incorporated. This splitting cannot be observed in the "as-prepared" sample, probably because the dopant ions are adhering as adsorbing species [16] and not incorporated in crystalline structure. The integral luminescence signal increases with one order of magnitude in the annealed samples and even more after sintering (Figure 5).

In the CaF_2 crystalline structure Eu^{3+} dopant ions can substitute for Ca^{2+} ions. Local charge compensation is realised by the interstitial F^- ions in nearest- neighbourhood forming tetragonal (C_{4v}) centers or by oxygen ions substituting a nearest-neighbor fluoride ion in the lattice along the [111] forming trigonal (C_{3v}) centers (denoted as G1 centers) [25,26].In order to extract information about the local environment around the Eu^{3+} ionwe applied group-theoretical arguments developed by Binnemans et al. [18] for solutions and polycrystalline samples by using the excitation spectra depicted in Figure 6, looking on the number of the peaks. As the $^5D_0 \leftrightarrow {}^7F_0$ transition occurs between non-degenerate levels their splitting shows the number of the non-equivalent Eu^{3+}-sites; the observation of this transition indicates one of the *(C_s), (C_n)* or *(C_{nV})* symmetries [18]. According to the site symmetry discrimination scheme, for the $^5D_0 \rightarrow {}^7F_{1,2,4}$ transitions on (C_{4v})and (C_{3v})coordination symmetry we expect one, two, three and one, two, two lines, respectively (as presented in Table 1) [18].

Table 1. Experimental PL excitation lines $^7F_0 - {}^5D_{0,1,2}$ (nm) of the 610 nm luminescence and the expected number of lines according to the point group (C_{2v}), (C_{3v}) and (C_{4v}) symmetries; weaker lines are marked with a star (*).

	$^7F_0 - {}^5D_0$	$^7F_0 - {}^5D_1$	$^7F_0 - {}^5D_2$
As-prepared	570 nm	525 nm	464 nm
400 or 800°C	573.5 nm	520, 522.5, 524.5 nm	460, 463, 465*, 468 nm
1300°C	573.5, 576 nm	520, 522.5, 524.5, 526.5 nm	460,463, 463.5*, 465, 468 nm
point group *(C_{4v})*	1	2	2
point group *(C_{3v})*	1	2	3
point group *(C_{2v})*	1	3	4

However the number of lines observed does not correspond to one of these coordination symmetries being consistent with a (C_{2v})one. Moreover, in the UV-excitation spectra (not shown) we have observed a broad and intense band at about 250nm assigned to the $O^{2-} \rightarrow Eu^{3+}$ inter-configurational charge-transfer (CT) [27] indicating the presence of oxygen ions in the Eu^{3+}-ion neighbourhood. Laser excited luminescence studies that have shownthe pairing of Eu^{3+}-ions with oxygen ions as Eu-O dimer centres, with orthorhombic symmetry [28].All these facts indicate the incorporation of the Eu^{3+} ions within the CaF_2 matrix with (C_{2v})coordination symmetry and with oxygen ions in the neighborhood.

The situation is different for the sintered samplewhere it is observed an increase of the luminescence signal with more than one order of magnitude due to the nanopowder densification through a mass transport controlled by diffusion [29]. Moreover, in PL excitation spectrum ($^7F_0 \rightarrow {}^5D_0$) a new peak emerges at 576 nm (Figure 6) indicating two non-equivalent Eu^{3+}-sites [18]. Because the transitionspeaks of each site superposed in the spectrum a simple straightforward determination is not possible [18].

3.5.Thermoluminescence

Structural and morphological evolutionsduring annealing of the on the Eu^{3+}-doped CaF_2 powder samples can be tracked by using thermoluminescence (TL) method as well. In Figure 8 are depicted the TL curves recorded on “as-prepared” and annealed samples by comparison to that recorded in CaF_2 commercial crystalline powder.

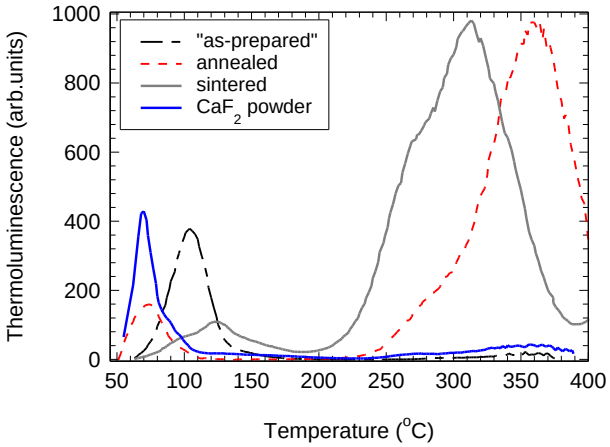

Fig. 7. Normalised TL curves recorded on Eu^{3+}-doped CaF_2 powder samples annealed at indicated temperatures; the curve recorded on CaF_2 commercial crystalline powder is also shown.

The basic TL model assumes that some of the charge carriers produced by irradiation (electrons and holes) are trapped in local energy levels (such as vacancies, interstitials, or impurities) within the band gap. During the heating, they are thermally released and recombine with carriers of the opposite sign, giving rise to TL. Thermal energy or activation energy corresponding to each glow peak represents the trap depth [30]. In the particular case of RE^{3+}-doped crystals, new energy levels are introduced by the doping and their location relative to the valence and conduction bands determine the characteristic behaviour of the ion as deep or shallow electron trap or as hole trap [31-33].

In the "as-prepared" powder sample we have observed only a peak at 105°C similar to the peak recorded at 70°C in polycrystalline CaF_2 powder (Figure 8). They have been assigned to the luminescent recombination of intrinsic defects in the CaF_2 structure. In the annealed samples new TL peaks emerge at high temperatures above 300°C due to the Eu^{3+}-ion incorporation in the CaF_2 crystalline structure. As this TL peaks are not observed in the "as-prepared" sample this indicates that the dopant ions are incorporated only after annealing, which is consistent with the PL measurements. The sample annealed at 800°C has shown a strong TL peak at 360°C but in the sintered sample we observed a TL peak at 310°C with a shoulder at about 260°C.It was shown that in calcium fluoride Eu^{3+} is a deep electron traps because after the electron capture it is transformed into Eu^{2+} ion with the ground level well below the conduction band [33]. Therefore the 360°C TL peak in the sample annealed at 800°C has been assigned to the thermal release of the electron from the Eu^{3+} traps followed by the recombination with the hole traps; there is only one Eu^{3+} site and therefore we observe only one TL peak. In the sintered sample the photoluminescence measurements have shown two non-equivalent Eu^{3+}-sites and therefore the two TL peaks has been assigned to the thermal release of the electrons from the Eu^{3+} traps in these two sites.

4. Conclusions

We have studied the influence of the thermal treatments on the structural, morphological and luminescence properties of the Eu^{3+}-doped CaF_2nanocrystalline powders synthesized by using aqueous co-precipitation technique.

Thermal treatments induce the incorporation into the CaF_2 phase of both Eu^{2+} and Eu^{3+}ion species at 438°C and at 635°C, respectively, probably through a diffusion-controlled mass transport mechanism similar to the sintering processes. This procedure induces a balance between Eu^{2+} and Eu^{3+} with the increasing of the Eu^{3+}/Eu^{2+} ratio at high temperatures.

The cathodoluminescence measurements showed uniform distribution of the europiumdopant ions in the nanoparticles in the annealed samples accompanied by an increase of the integral luminescence signal with about one order of magnitude and even more in the sintered samples.The presence of Eu^{3+} in CaF_2 nanocrystals is marked by the changing of shapes from cubic to spherical. This fact is consistent with the thermal analysis results in which, at higher

temperatures, Eu^{3+} ions are incorporated in CaF_2 crystalline structures as Eu^{3+}-O dimmers. The orthorhombic structure of α-EuF_3 combined with the cubic structure of CaF_2 induces the spherical shape of the nanocrystals.

Photoluminescence measurements and group-theoretical arguments support the above ideathat in the annealed sample the Eu^{3+}-ions associate with oxide ions in the form of Eu^{3+}-O dimer centre with the coordination symmetry (C_{2v}). In the sintered samples we have observed two non-equivalent sites and an increase of the luminescence signal with more than one order of magnitude due to the nanopowder densification.

TL peaks have been observed at 360^{o}C in annealed sample and at 260 and 310^{o}C in the sintered one. They have been assigned to the recombination of the electrons thermal released from the Eu^{3+} traps in (Eu^{3+}-O) dimer centre or in two non-equivalent sites, respectively.

Acknowledgements

The authors gratefully acknowledge the financial support of UEFISCDI through projects IDEI Project no. 290/05.11.2011 and TE code PN-II-RU-TE-2011-3-0107(contract 37/2011). We are also grateful to Dr. Elena Apostol for the assistance in the preparation of the samples.

References

[1] H. Schäfer, M. Haase, Angew. Chem. Int. Ed.**50,** 5808 (2011)
[2] V.K. Tikhomirov, M. Mortier, P.Gredin, G. Patriarche, C. Görller-Walran, V.V. Moshchalkov,Optics Express**16** (19) 14544 (2008)
[3] S.Heer, K. Kömpe, H.U.Güdel, M.Haase, Advanced Materials **16** 2102 (2004)
[4] A.Bednarkiewicz, D.Wawrzynczyk, M.Nyk, W.Strek,Optical Materials **33** 1481 (2011)
[5] H. S Mader, P.Kele, S. M Saleh, O. S Wolfbeis,Current Opinion in Chemical Biology **14** 582 (2010)
[6] J.Lellouche, A. Friedman, J.-P.Lellouche, A.Gedanken, E.Banin,Nanomedicine Nanotechnology, Biology and Medicine **8**(5) 702 (2012)
[7] V.S. Kortov, Radiation Measurements m**45** 512 (2010)
[8] P. P. Fedorov, A. A. Luginina, S.V. Kuznetsov, V. V. Osiko, Journal of Fluorine Chemistry **132** 1012 (2011) -1039
[9] M.M. Lezhnina, H. Kaetker, U.H. Kynast, Optical Materials **30** 264 (2007)
[10] C. Li, J. Lin, Journal of Materials Chemistry **20** 6831 (2010)
[11] P. Samuel, H. Ishizawa, Y. Ezura, K. Ichi Ueda, S. MoorthyBabu, Optical Materials **33** 735 (2011)
[12] M.Sh. Akchurin,T.T. Basiev,A.A. Demidenko,M.E. Doroshenko,P.P. Fedorov, E.A. Garibin,P.E. Gusev,S.V. Kuznetsov,M.A. Krutov,I.A. Mironov,V.V. Osiko, P.A. Popov,Optical Materials **35**(3) 444 (2013)
[13] Tao Jiang, Weiping Qin, Dan Zhao,Materials Letters **74** 54 (2012)
[14] Y. Li, T. Liu, Y. Du, Applied Physics Express **5,** 086501 (2012)
[15] Z. Yang, G. Wang, Y.Guo, F. Kang, Y. Huang, D. Bo,Materials Research Bulletin **47** 3965 (2012)
[16] F. Wang, X. Fan, D. Pi, M. Wang, Solid State Communications,**133** 775 (2005)
[17] J. Labéqueria, P. Gredin, M. Mortier, G. Patriarche, A. De Kozak,ZeitschriftfürAnorganische und AllgemeineChemie **632** 1538 (2006)
[18] K. Binnemans, C. Görller-Walrand, Journal of Rare Earths **14** 173 (1996)
[19] K. Driesen, V.K. Tikhomirov, C. Görller-Walrand, Journal of Applied Physics **102** 024312 (2007)
[20] Yu. N. Orlov, V. E. Bozhevolnov, L.N. Ivanov, V.I.Sluev, S.K. Obyden, G.V. Saparin, G.V. Spivac, V.V. Karelin, Journal of Crystal Growth, **49,** 109 (1980)
[21] W. Hume-Rothery, H. M. Powell, ZeitschriftfürKristallographie, **91,** 23 (1935)
[22] H. Okamoto, Journal of Phase Equilibria and Diffusion, **31,** 495 (2010)
[23] A. L. Patterson, Physical Reviews, **56** 978 (1939)
[24] T. Kobayasi, S. Mroczkowski, J. F. Owen,Journal of Luminescence, **21**, 247 (1980)
[25] S.W.S. McKeever, M.D. Brown, T.J. Abbundi, H. Chan, V.K. Mathur, Journal of Applied

Physics **60** 2505 (1986)
[26] P. Dorenbos, H.W. den Hartog, Physical Reviews B **31** 3932 (1985)
[27] G. Blasse, B. C. Grabmaier, Luminescent Materials, p.10. Springer-Verlag, Berlin, Germany(1994)
[28] D. Van Der Voort, G.J. Dirksen, G. Blasse, Journal of Physics and Chemistry of Solids, **53** 219 (1992)
[29] B. C. Grabmaier, W. Rossner, Nuclear Tracks and Radiation Measurements **21** 43 (1993)
[30] S. W. S. McKeever, Thermoluminescenceof Solids, Cambridge University Press, New York, USA (1985)
[31] P. A. Rodnyi, I. V. Khodyuk, G. B. Stryganyuk, Physics of the Solid State **50** 1639 (2008)
[32] P.Dorenbos,A.J.J. Bos,Radiation Measurements **43** 139 (2008)
[33] P. Dorenbos, Journal of Physics: Condensed Matter **15** 4797 (2003)